
A Comparison of EGF and MAb 528 Labeled with ^{111}In for Imaging Human Breast Cancer

Raymond M. Reilly, Reza Kiarash, Jasbir Sandhu, Ying Wai Lee, Ross G. Cameron, Aaron Hendler, Katherine Vallis, and Jean Gariépy

Division of Nuclear Medicine and Departments of Pathology and Radiation Oncology, Toronto General Hospital/Princess Margaret Hospital, University Health Network, Toronto; Samuel Lunenfeld Research Institute, Mount Sinai Hospital, Toronto; and Departments of Medical Imaging, Pharmaceutical Sciences, Radiation Oncology, and Medical Biophysics, University of Toronto, Toronto, Canada

Our objective was to compare ^{111}In -labeled human epidermal growth factor (hEGF), a 53-amino acid peptide with anti-epidermal growth factor receptor (EGFR) monoclonal antibody (MAb) 528 (IgG_{2a}) for imaging EGFR-positive breast cancer.

Methods: hEGF and MAb 528 were derivatized with diethylenetriamine pentaacetic acid (DTPA) and labeled with ^{111}In acetate. Receptor binding assays were conducted in vitro against MDA-MB-468 human breast cancer cells. Biodistribution and tumor imaging studies were conducted after intravenous injection of the radiopharmaceuticals in athymic mice bearing subcutaneous MCF-7, MDA-MB-231, or MDA-MB-468 human breast cancer xenografts or in severe combined immunodeficiency mice implanted with a breast cancer metastasis (JW-97 cells). MCF-7, MDA-MB-231, JW-97, and MDA-MB-468 cells expressed 1.5×10^4 , 1.3×10^5 , 2.7×10^5 , and 1.3×10^6 EGFR/cell, respectively in vitro. **Results:** ^{111}In -DTPA-hEGF and ^{111}In -DTPA-MAb 528 bound with high affinity to MDA-MB-468 cells (K_d of 7.5×10^8 and 1.2×10^8 L/mol, respectively). ^{111}In -DTPA-hEGF was eliminated rapidly from the blood with $< 0.2\%$ injected dose/g (%ID/g) circulating at 72 h after injection, whereas ^{111}In -DTPA-MAb 528 was cleared more slowly (3 %ID/g in the blood at 72 h). Maximum localization of ^{111}In -DTPA-hEGF in MDA-MB-468 tumors (2.2 %ID/g) was 10-fold lower than with ^{111}In -DTPA-MAb 528 (21.6 %ID/g). There was high uptake in the liver and kidneys for both radiopharmaceuticals. Tumor-to-blood ratios were greater for ^{111}In -labeled hEGF than for MAb 528 (12:1 versus 6:1), but all other tumor-to-normal tissue ratios were higher for MAb 528. MDA-MB-468 and JW-97 tumors were imaged successfully with both radiopharmaceuticals, but tumors were more easily visualized using ^{111}In -labeled MAb 528. There was no direct quantitative relationship between EGFR expression on breast cancer cell lines in vitro, and tumor uptake of the radiopharmaceuticals in vivo, but control studies showed that tumor uptake was receptor mediated. **Conclusion:** Our results suggest that the tumor uptake in vivo of receptor-binding radiopharmaceuticals is controlled to a greater extent by their elimination rate from the blood than by the level of receptor expression on the cancer cells. Radiolabeled anti-EGFR MAbs would be more effective for tumor imaging in cancer patients than peptide-based radiopharmaceuticals such as hEGF, because they exhibit higher tumor uptake at only moderately lower tumor-to-blood ratios.

Key Words: breast cancer; epidermal growth factor; monoclonal antibody 528; ^{111}In ; imaging; epidermal growth factor receptor

J Nucl Med 2000; 41:903–911

The overexpression of cell surface receptors for peptide growth factors is believed to be one process whereby cancer cells acquire the ability to escape normal growth regulatory mechanisms. The presence of the epidermal growth factor receptor (EGFR) at levels up to 100 times higher than on most normal epithelial tissues ($< 10^4$ receptors/cell) has been observed in 30%–60% of human breast cancers (1). EGFR overexpression in breast cancer is inversely correlated with estrogen receptor (ER) expression and is directly correlated with a lack of response to hormonal therapy with tamoxifen. Several studies have associated this cellular phenotype with poor long-term survival [studies reviewed by Klijn et al. (1)].

Patients with disseminated, hormone-resistant breast cancer are candidates for systemic chemotherapy. In addition, new drugs are currently under development that would specifically target the high levels of EGFR expression commonly observed in such malignancies. These drugs include monoclonal antibodies (MAbs) that block the binding of epidermal growth factor (EGF) to the receptor (2), tyrosine kinase inhibitors (tyrphostins) that can interfere with the intracellular signaling pathways (3), and EGF-conjugated toxins that specifically deliver highly potent inhibitors of protein synthesis into the cytoplasm of the cancer cells (4). A logical extension of this strategy, currently being explored in our laboratory (5) and by others (6), would be to develop novel radiotherapeutic agents that could deliver high doses of radiation specifically to EGFR-positive cancer cells.

The effectiveness of new therapeutic agents targeted to the EGFR will depend on the ability to detect and characterize EGFR-expressing metastatic lesions throughout the body. ER status is commonly measured in biopsies of primary breast cancer lesions at the time of staging to select patients for hormonal therapy. EGFR expression in metastatic disease could be inferred from the inverse correlation

Received Apr. 14, 1999; revision accepted Aug. 9, 1999.

For correspondence or reprints contact: Raymond M. Reilly, PhD, Division of Nuclear Medicine, Toronto General Hospital, 585 University Ave., Toronto, Ontario, M5G 2C4 Canada.

between ER and EGFR expression in breast cancer. This approach may be limited, however, by potential differences in EGFR/ER positivity between the primary tumor and metastases, heterogeneity in receptor expression by the tumor cells, temporal changes in ER/EGFR expression that can occur as a result of treatment (7), and the inability to directly evaluate EGFR expression in individual lesions. A survey of the whole body with γ scintigraphy using radiopharmaceuticals specifically targeted to the EGFR would be useful to detect breast cancer lesions and characterize the level of EGFR expression at these sites to appropriately select patients for novel anti-EGFR therapies.

It has been proposed that peptide-based radiopharmaceuticals, such as radiolabeled growth factors, may be more effective for imaging tumors than radiolabeled MABs (8), because of more rapid elimination from the blood and higher tumor-to-blood ratios at early time points. The objective of this study therefore was to directly compare human EGF (hEGF), a 53-amino acid peptide ligand for the EGFR, with antiEGFR MAB 528 (9) labeled with ^{111}In for imaging EGFR-positive human breast cancer.

MATERIALS AND METHODS

Breast Cancer Cells

MDA-MB-468 and MDA-MB-231 human breast cancer cells were obtained from the American Type Culture Collection (ATCC, Rockville, MD) and were cultured in L-15 medium (Sigma, St. Louis, MO) supplemented with 10% fetal calf serum (FCS). MCF-7 breast cancer cells were obtained from Dr. A. Marks at the Banting and Best Department of Medical Research, University of Toronto (Toronto, Ontario, Canada) and were cultured in minimal essential medium (MEM, Sigma) supplemented with 10% FCS, nonessential amino acids, and glutamine (Gibco-BRL, Life Technologies, Burlington, Ontario, Canada). S1 breast cancer cells are a subclone of the MDA-MB-468 breast cancer cell line and express a lower number of EGFR molecules on their surface (10). S1 cells were obtained from Dr. R. Buick at the Ontario Cancer Institute (Toronto, Ontario, Canada) and were cultured in L-15 medium supplemented with 10% FCS and 100 nmol/L nEGF. JW-97 human breast cancer cells were obtained by trypsinization of a skeletal metastasis from a patient with advanced disease and then passaged in severe combined immunodeficiency (scid) mice. JW-97 cells were cultured in RPMI 1640 medium (Sigma) supplemented with 10% FCS.

Radiolabeling of EGF

hEGF (Upstate Biotechnology, Lake Placid, NY) was derivatized with diethylenetriamine pentaacetic acid (DTPA) using the bicyclic anhydride of DTPA (Sigma) as previously described (11). DTPA-derivatized hEGF showed a single band with an apparent molecular weight (M_r) of 6 kDa by sodium dodecylsulfate polyacrylamide gel electrophoresis (SDS-PAGE) on a tris-Tricine gel (BioRad, Mississauga, Ontario, Canada), indicating no apparent cross-linking of hEGF molecules after reaction with the bicyclic DTPA anhydride. DTPA-conjugated hEGF (25–50 μg) was radiolabeled with ^{111}In -acetate to a specific activity of 3.7–7.4 MBq/ μg (22,200–44,400 MBq/ μmol). ^{111}In -acetate was prepared by mixing equal volumes of ^{111}In -chloride (>7,400 MBq/mL; MDS-Nordion, Kanata, Ontario, Canada) and 1 mol/L acetate buffer pH 6.

^{111}In -DTPA-hEGF was purified from free ^{111}In by size-exclusion chromatography on a P-2 mini-column (BioRad), then analyzed for radiochemical purity by silica gel instant thin-layer chromatography (ITLC-SG; Gelman, Ann Arbor, MI) in 100 mmol/L sodium citrate pH 5. The radiolabeling efficiency was ~80%. The radiochemical purity of ^{111}In -DTPA-hEGF was routinely between 95% and 98%.

hEGF was radioiodinated to a specific activity of 1.5–2.2 MBq/ μg (8,880–13,320 mCi/ μmol) by incubating 10 μg hEGF with 18.5–37 MBq ^{125}I -sodium iodide (Nycomed-Amersham, Oakville, Ontario, Canada) and 20 μg chloramine-T (Sigma) for 30 s in a glass tube at room temperature. After addition of sodium metabisulfite (40 μg), the radioiodinated hEGF was purified on a P-2 mini-column. The radiolabeling efficiency was ~70%. The radiochemical purity of ^{125}I -hEGF was >95%, as determined by paper chromatography (Whatman, Maidstone, UK) in 85% methanol.

Production and Radiolabeling of MAB 528

HB 8509 hybridoma cells secreting anti-EGFR MAB 528 (IgG_{2a}) were obtained from ATCC and were cultured in RPMI 1640 supplemented with 20% FCS. BALB/c mice were injected intraperitoneally with 1 mL Pristane (2,6,10,14-tetramethylpentadecane; Sigma), followed 3–4 d later with an intraperitoneal injection of 10^7 HB 8509 hybridoma cells in culture medium. After 2 wk, the ascites fluid was removed from the peritoneal cavity, and anti-EGFR MAB 528 was purified from the ascites fluid on a Protein G column (Pierce, Rockford, IL). The purified MAB 528 was desalted on a Sephadex G-25 column (PD-10; Pharmacia, Uppsala, Sweden), concentrated on a Centricon-30 ultrafiltration device (Amicon, Beverly, MA) and diluted to a concentration of 10 mg/mL in 50 mmol/L sodium bicarbonate buffer pH 7.5. The purity of the MAB 528 preparation was assessed by SDS-PAGE under nonreducing conditions on a 4%–20% tris-glycine gel (BioRad). The protein preparation resulted in a single band migrating with an apparent M_r of 150 kDa. Approximately 2 mg MAB 528 were obtained per milliliter of ascites fluid.

MAB 528 (0.5–1 mg), 10 mg/mL in trace-metal free 50 mmol/L sodium bicarbonate buffer pH 7.5 were derivatized with DTPA, using the bicyclic anhydride of DTPA (cDTPAA; Sigma) at a molar ratio (cDTPAA:MAB 528) of 10:1 as previously described (12). DTPA-MAB 528 was purified by size-exclusion chromatography on a Sephadex G-50 (Pharmacia) mini-column eluted with 50 mmol/L sodium bicarbonate buffer pH 7.5 followed by ultrafiltration through a Centricon-30 device. Analysis of DTPA-MAB 528 by SDS-PAGE under nonreducing conditions on a 4%–20% tris-glycine gel showed a predominant band with an apparent M_r of 150 kDa and a minor band with apparent M_r of 300 kDa, indicating a small proportion (<10%) of MAB 528 molecules cross-linked through cDTPAA. DTPA-MAB 528 (250–500 μg) was radiolabeled to a specific activity of 0.07–0.14 MBq/ μg (11,100–22,200 MBq/ μmol) with ^{111}In -acetate (37 MBq) and purified from free ^{111}In on a Sephadex G-50 mini-column eluted with 150 mmol/L sodium chloride. The radiolabeling efficiency of DTPA-MAB 528 was ~85%. The radiochemical purity of ^{111}In -DTPA-MAB 528 was routinely >95% determined by ITLC-SG developed in 100 mmol/L sodium citrate pH 5. A nonspecific murine IgG_{2a} (product no. M-9144; Sigma) was derivatized with cDTPAA and radiolabeled with ^{111}In -acetate in an identical manner to MAB 528.

MAB 528 (25–50 μg) was radioiodinated to a specific activity of 0.18–0.37 MBq/ μg (27,750–55,500 MBq/ μmol) by incubation with 18.5 MBq ^{125}I -sodium iodide in a glass tube precoated with 20 μg

1,3,4,6-tetrachloro-3 α ,6 α -diphenylglycouril (Sigma) at room temperature. Radioiodinated MAb 528 was purified on a Sephadex G-50 mini-column. The radiolabeling efficiency was ~70%. The radiochemical purity of ¹²⁵I-MAb 528 was >95% as determined by paper chromatography (Whatman No. 1) in 85% methanol.

Measurement of Receptor Binding In Vitro

The binding of radiolabeled hEGF or MAb 528 to its receptor on MDA-MB-468, S1, MDA-MB-231, MCF-7, or JW-97 human breast cancer cells was measured using a direct binding assay. Briefly, aliquots of either radiolabeled hEGF (0.25–80 ng) or MAb 528 (6 ng–4 μ g) were dispensed into 35-mm multiwell culture dishes containing $1.5\text{--}7 \times 10^6$ breast cancer cells in 1 mL of 150 mmol/L sodium chloride containing 0.2% weight/volume human serum albumin. After incubation of the dishes at 37°C for 30 min, the cells were transferred to tubes and centrifuged to separate the bound radioactivity (B) in the cell pellet from the free radioactivity (F) in the supernatant. The cell pellet and supernatant were counted in a γ scintillation counter (Packard Auto Gamma 5650; Packard Instruments, Downer's Grove, IL). Nonspecific binding was determined by conducting the assay in the presence of 100 nmol/L hEGF or MAb 528. The affinity constant (K_a) and number of receptors/cell (B_{\max}) were determined from a nonlinear fitting of the binding data (13).

The receptor-binding fraction (RBF) at infinite receptor excess was determined by incubating 0.5–1 ng ¹¹¹In-DTPA-hEGF or 10–20 ng ¹¹¹In-DTPA-MAb 528 with increasing concentrations of MDA-MB-468 breast cancer cells ($1\text{--}20 \times 10^6$ cells/mL) for 30 min at 37°C and determining the fraction of radioactivity bound. The RBF at infinite receptor excess was obtained from the intercept on the ordinate (1/RBF) of a plot of total/bound counts versus 1/cell concentration, as previously described by Lindmo et al. (14).

Biodistribution and Tumor Imaging Studies

Female, Swiss athymic (nu/nu) mice (4–6 wk old; Charles River Laboratories, Montreal, Quebec, Canada) were injected subcutaneously in the right hind leg with $5 \times 10^6\text{--}10^7$ MDA-MB-468, MDA-MB-231, or MCF-7 human breast cancer cells in growth medium. Mice inoculated with MCF-7 cells also received estradiol supplementation with biweekly subcutaneous injections of 0.5 mg conjugated estrogens (Premarin; Wyeth-Ayerst, St. Laurent, Quebec, Canada), which are required for MCF-7 cells to form tumor xenografts. A freshly obtained biopsy of a skeletal metastasis from a patient with advanced breast cancer (JW-97 cells) was implanted in the left hind leg of scid mice (Samuel Lunenfeld Research Institute). A dose of 1.85–3.7 MBq ¹¹¹In-DTPA-hEGF (0.5–1 μ g) or ¹¹¹In-DTPA-MAb 528 (25–50 μ g) was injected intravenously into mice when the tumors reached a diameter of 0.25–0.5 cm (1–2 cm for JW-97 tumors). One group of control mice received a dose of

1.85–3.7 MBq ¹¹¹In-DTPA (DraxImage, Dorval, Quebec, Canada). An ¹¹¹In-labeled nonspecific murine IgG_{2a} was injected into a second group of control mice, whereas ¹¹¹In-DTPA-hEGF premixed with 500 μ g nonradioactive hEGF (ratio of nonradioactive hEGF-to-¹¹¹In-DTPA-hEGF = 1000:1) was injected intravenously into a third group of control mice.

At 24, 48, and 72 h after injection, groups of mice were killed by cervical dislocation, and the tumor and samples of normal tissues were removed to measure levels of radioactivity. Tissue samples were weighed and counted along with a standard of the injected radiopharmaceutical in a γ counter (Packard Auto Gamma 5650; Packard Instruments) using a window (150–270 keV) to include the 2 γ photopeaks of ¹¹¹In (172 and 247 keV). The uptake of each radiopharmaceutical by the tumor and normal tissue was expressed as percentage injected dose per gram (%ID/g) of tissue and as tumor-to-normal tissue ratios (T/NT). At 72 h after injection, posterior images of the mice implanted with the MDA-MB-468, JW-97, or MCF-7 human breast cancer xenografts were obtained with a Siemens ZLC-3700 γ camera (Siemens, Knoxville, TN) fitted with a medium-energy, pinhole collimator and interfaced to a General Electric Star 4000i computer (General Electric, Milwaukee, WI). Images were acquired for 10 min using a 20% window centered over the 172 and 247 keV photopeaks of ¹¹¹In. Animal studies were conducted under an approved Animal Care Protocol (#94-036) at The Toronto Hospital and following the Canadian Council on Animal Care (CCAC) guidelines.

Statistical Analysis

Statistical comparisons were performed by ANOVA (F-test, $P < 0.05$) and Student *t* test ($P < 0.05$).

RESULTS

Binding of Radiolabeled hEGF and MAb 528 to Breast Cancer Cells In Vitro

¹¹¹In-DTPA-hEGF and ¹¹¹In-DTPA-MAb 528 bound with high affinity and specificity in vitro to MDA-MB-468 human breast cancer cells (Table 1). K_a was ~6-fold higher for ¹¹¹In-DTPA-hEGF than for ¹¹¹In-DTPA-MAb 528. There was no significant difference in binding affinity between ¹¹¹In- and corresponding ¹²⁵I-labeled analogs, suggesting that the conjugation of the DTPA chelator to amino groups and their radiolabeling with ¹¹¹In did not adversely effect the binding of the resulting radiopharmaceutical to the EGFR. The number of binding sites recognized on the MDA-MB-468 cells (B_{\max}) was similar for all 4 radiolabeled ligands. There was no significant difference ($P = 0.0847$) in the

TABLE 1
Comparison of Binding of ¹¹¹In- and ¹²⁵I-Labeled hEGF or MAb 528 to MDA-MB-468 Human Breast Cancer Cells

Characteristic	¹¹¹ In-DTPA-hEGF	¹²⁵ I-hEGF	¹¹¹ In-DTPA-MAb 528	¹²⁵ I-MAb 528
No. of experiments	6	10	5	4
K_a (L/mol)*	$7.5 \pm 3.8 \times 10^8$	$7.3 \pm 3.6 \times 10^8$	$1.2 \pm 0.6 \times 10^8$	$9.4 \pm 2.0 \times 10^7$
B_{\max} (sites/cell)†	$1.3 \pm 0.3 \times 10^6$	$7.2 \pm 0.3 \times 10^5$	$9.0 \pm 4.5 \times 10^5$	$7.0 \pm 3.8 \times 10^5$

*Affinity constant mean \pm SD.

†Maximum number of binding sites/cell (mean \pm SD).

fraction of radiolabeled molecules able to bind to EGFRs on MDA-MB-468 cells under conditions of infinite receptor excess for $^{111}\text{In-DTPA-hEGF}$ (0.73 ± 0.17 ; $n = 3$) and $^{111}\text{In-DTPA-MAb 528}$ (0.50 ± 0.04 ; $n = 3$).

EGFR expression varied considerably among the 5 breast cancer cell lines tested (Table 2). The highest expression ($>10^6$ EGFR/cell) was observed on MDA-MB-468 cells, which have an amplified EGFR gene (10). MCF-7 and S1 cells exhibited the lowest expression ($<10^4$ EGFR/cell). MCF-7 is an ER-positive cell line, expected to have low EGFR expression, and the cell line S1 represents a subclone of the MDA-MB-468 cell line, in which the expression of the EGFR gene is downregulated (10). JW-97 cells, originally obtained from a biopsy of a skeletal metastasis in a patient with advanced disease, exhibited intermediate levels of EGFR expression, similar to the levels on the MDA-MB-231 breast cancer cell line ($1-3 \times 10^5$ receptors/cell) but almost 30-fold higher than on most normal epithelial tissues ($<10^4$ EGFR/cell).

Biodistribution and Tumor Imaging Studies

The biodistribution of $^{111}\text{In-DTPA-hEGF}$ and $^{111}\text{In-DTPA-MAb 528}$ at selected times after an intravenous (tail vein) injection in athymic mice bearing subcutaneous MDA-MB-468 human breast cancer xenografts is shown in Figure 1. The blood levels of $^{111}\text{In-DTPA-hEGF}$ (Fig. 1A) decreased rapidly with <0.8 %ID/g present in the blood at 24 h after injection, decreasing to <0.2 %ID/g at 72 h. Assuming a blood volume of ~ 2.5 mL for a mouse weighing 25 g, the concentration of $^{111}\text{In-DTPA-hEGF}$ in the blood corresponded to about 1.7%–2.5% of the injected dose of the radiopharmaceutical at 24 h and $<0.5\%$ at 72 h. In contrast, the blood levels of $^{111}\text{In-DTPA-MAb 528}$ (Fig. 1B) decreased more slowly with ~ 9 %ID/g present in the blood at 24 h after injection, decreasing to 3 %ID/g at 72 h. The concentration of $^{111}\text{In-DTPA-MAb 528}$ in the blood corresponded to about 21%–25% of the injected dose of the radiopharmaceutical circulating at 24 h after injection, decreasing to about 7%–8% at 72 h.

The normal tissues that accumulated the highest concentrations of the radiopharmaceuticals were the liver and kidneys (Fig. 1). Liver uptake of $^{111}\text{In-DTPA-hEGF}$ (Fig. 1A) was relatively constant, ranging from 8 to 10 %ID/g. The concentration of $^{111}\text{In-DTPA-hEGF}$ in the kidneys increased slightly from about 11 %ID/g at 24 h to 14 %ID/g at 72 h after injection. Approximately 11%–14% of the injected dose of $^{111}\text{In-DTPA-hEGF}$ localized in the liver and 4%–5% in the kidneys, assuming organ weights of 1.4 and 0.36 g, respectively. For $^{111}\text{In-DTPA-MAb 528}$ (Fig. 1B), liver accumulation ranged from 6 to 8 %ID/g and uptake in the kidneys was 12–17 %ID/g over the time period of 24–72 h after injection. The liver sequestered $\sim 8\%$ – 11% of the injected dose of $^{111}\text{In-DTPA-MAb 528}$, and the kidneys accumulated 4%–6%. There were no significant differences in the concentrations of the 2 radiopharmaceuticals in the liver or kidneys at 72 h.

Maximum localization of $^{111}\text{In-DTPA-hEGF}$ in the MDA-MB-468 human breast cancer xenografts occurred at 72 h after injection (2.2 %ID/g) and was up to 10-fold lower than that observed for $^{111}\text{In-DTPA-MAb 528}$ (Fig. 1). Maximum tumor uptake of $^{111}\text{In-DTPA-MAb 528}$ occurred at 24 h after injection (21.6 %ID/g), then decreased to 11–15 %ID/g at 48–72 h after injection. The mean uptake of $^{111}\text{In-DTPA-hEGF}$ in the MDA-MB-468 breast cancer xenografts at 72 h after injection was decreased more than 5-fold by co-administering 500 μg of unlabeled hEGF (0.40 ± 0.15 %ID/g), suggesting that tumor uptake was a receptor-mediated event. Similarly, the uptake of nonspecific $^{111}\text{In-labeled IgG}_{2a}$ into MDA-MB-468 breast cancer xenografts at 72 h after injection (9.13 ± 1.92 %ID/g) was 2-fold lower than that observed for $^{111}\text{In-DTPA-MAb 528}$, suggesting that uptake of MAb 528 by tumor cells was also receptor mediated. The mean tumor uptake of $^{111}\text{In-DTPA}$ at 72 h after injection was 0.07 ± 0.01 %ID/g.

T/NTs at selected times after administration of the radiopharmaceuticals are shown in Figure 2. Tumor-to-blood ratios increased rapidly for $^{111}\text{In-DTPA-hEGF}$ (Fig. 2A), reaching values of 2.6:1 at 24 h and increasing to 12:1

TABLE 2
Tumor Localization of $^{111}\text{In-DTPA-hEGF}$ and $^{111}\text{In-DTPA-MAb 528}$ at 72 Hours After Injection as Function of EGFR Expression

Breast cancer xenograft†	EGFR expression‡ (receptors/cell $\times 10^5$)	Tumor uptake* (%ID/g)	
		$^{111}\text{In-DTPA-hEGF}$	$^{111}\text{In-DTPA-MAb 528}$
MCF-7	0.15 ± 0.07	1.95 ± 0.56	8.40 ± 1.60
MDA-MB-231	1.33 ± 0.85	1.46 ± 0.89	18.03 ± 7.87
JW-97	2.71 ± 0.83	0.70 ± 0.07	4.90 ± 1.08
MDA-MB-468	12.80 ± 2.99	2.24 ± 0.32	15.35 ± 2.49

*Mean \pm SEM of 3–6 animals per experiment.
†MCF-7, MDA-MB-231, and MDA-MB-468 xenografts were hosted in athymic mice. JW-97 xenografts were hosted in scid mice.
‡EGFR expression determined in vitro with $^{111}\text{In-DTPA-hEGF}$. Mean \pm SD of 3–10 experiments.

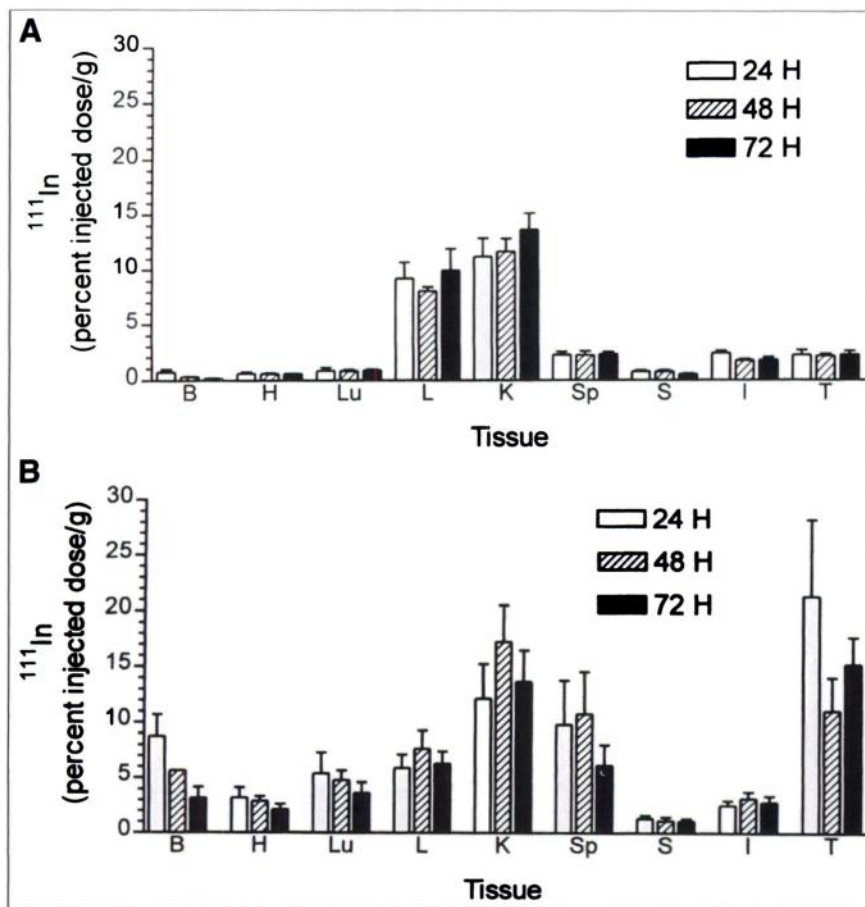


FIGURE 1. Biodistribution at selected times after administration of ^{111}In -DTPA-hEGF (A) and ^{111}In -DTPA-MAb 528 (B) in athymic mice bearing subcutaneous MDA-MB-468 human breast cancer xenografts. Tissues shown are blood (B), heart (H), lungs (Lu), liver (L), kidneys (K), spleen (Sp), stomach (S), intestines (I), and tumor (T).

at 72 h after injection. Tumor-to-blood ratios for ^{111}In -DTPA-MAb 528 (Fig. 2B) increased more slowly, from 2.5:1 at 24 h to about 6:1 at 72 h after injection. T/NTs for ^{111}In -DTPA-hEGF were $>2:1$ for blood, heart, lungs, stomach, and intestine up to 72 h after injection but were $<1:1$ for the liver and kidneys as a result of high accumulation of radiopharmaceutical in these normal tissues. Except for the blood, all other T/NTs for ^{111}In -DTPA-MAb 528 were higher than those for ^{111}In -DTPA-hEGF (Fig. 2B). Tumor-to-liver ratios for ^{111}In -DTPA-MAb 528 (1.4:1–3.3:1) were 5- to 11-fold higher than those observed for ^{111}In -DTPA-hEGF, and tumor-to-kidney ratios were 3- to 10-fold greater (0.7:1–1.8:1).

Biodistribution studies in athymic or scid mice bearing subcutaneous MDA-MB-468, MDA-MB-231, JW-97, or MCF-7 human breast cancer xenografts at 72 h after injection of ^{111}In -DTPA-hEGF or ^{111}In -DTPA-MAb 528 showed no direct correlation between the level of tumor uptake of the radiopharmaceuticals and the level of EGFR expression on these cell lines measured in vitro (Table 2). For example, there were no significant differences in the level of accumulation of ^{111}In -DTPA-hEGF (or ^{111}In -DTPA-MAb 528) in MCF-7 or MDA-MB-468 breast cancer xenografts, despite a 100-fold difference in receptor expression ($P = 0.6408$ and $P = 0.0957$, respectively). Similarly,

there were no significant differences in the level of accumulation of ^{111}In -DTPA-hEGF (or ^{111}In -DTPA-MAb 528) in MDA-MB-231 and MDA-MB-468 breast cancer xenografts, despite a 10-fold difference in receptor expression ($P = 0.3955$ and $P = 0.6838$, respectively). Nevertheless, the tumor uptake of ^{111}In -DTPA-MAb 528 was 4- to 12-fold higher than that of ^{111}In -DTPA-hEGF in all cases. The localization of either ^{111}In -DTPA-hEGF or ^{111}In -DTPA-MAb 528 was significantly lower in JW-97 tumors than in the MDA-MB-468 breast cancer xenografts ($P = 0.0041$ and $P = 0.0260$, respectively). There was no significant difference in the tumor uptake of ^{111}In -DTPA-hEGF in MDA-MB-231 breast cancer xenografts compared with the JW-97 tumors ($P = 0.427$). Similarly, there was no significant difference in the tumor uptake of ^{111}In -DTPA-MAb 528 between the MDA-MB-231 or JW-97 tumor xenografts ($P = 0.684$).

MDA-MB-468 and JW-97 human breast cancer xenografts expressing 1.3×10^6 or 2.7×10^5 EGFR/cell in vitro, respectively, (Table 1) were successfully imaged with ^{111}In -DTPA-hEGF or ^{111}In -DTPA-MAb 528 at 72 h after injection (Figs. 3 and 4). However, the greater tumor uptake of ^{111}In -DTPA-MAb 528 compared with ^{111}In -DTPA-hEGF resulted in an enhanced definition of the breast cancer xenografts. The liver and kidneys were the major normal

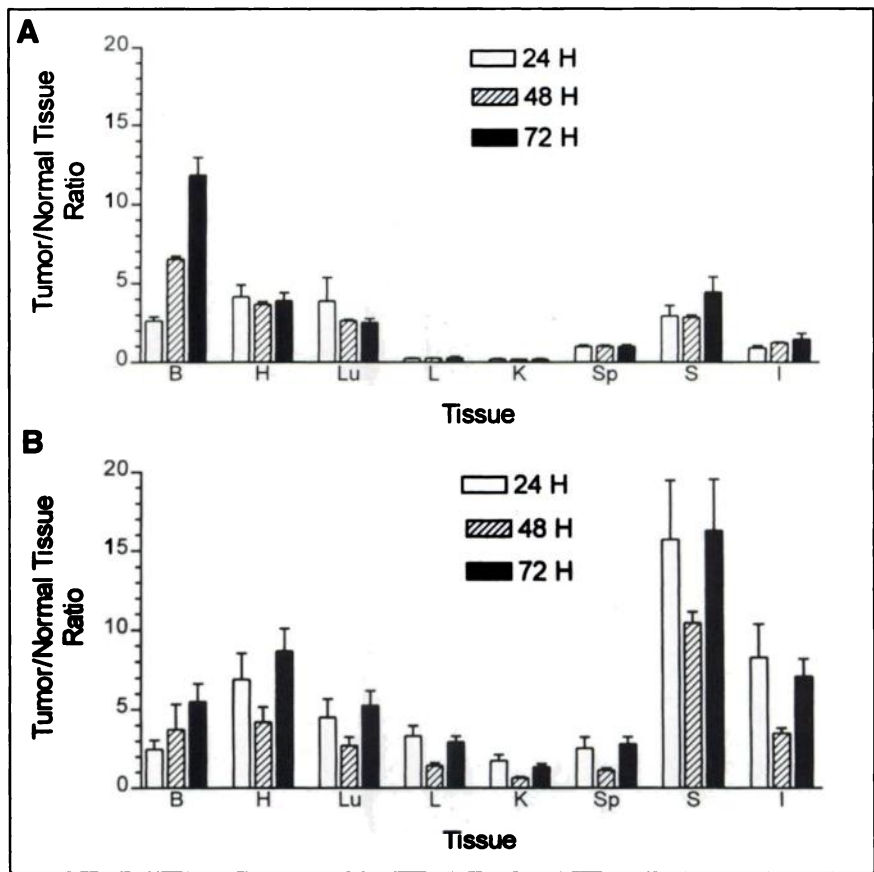


FIGURE 2. T/NTs at selected times after administration of ^{111}In -DTPA-hEGF (A) and ^{111}In -DTPA-MAb 528 (B) in athymic mice bearing subcutaneous MDA-MB-468 human breast cancer xenografts. Tissues shown are blood (B), heart (H), lungs (Lu), liver (L), kidneys (K), spleen (Sp), stomach (S), and intestines (I).

organs visualized on the images, but there was also some uptake in the area of the submaxillary glands. The levels of circulating radioactivity and whole-body radioactivity were considerably lower on the images obtained using ^{111}In -DTPA-

hEGF than on those obtained with ^{111}In -DTPA-MAb 528. MCF-7 xenografts could not be visualized with either ^{111}In -DTPA-hEGF or ^{111}In -DTPA-MAb 528 because of their small size (<0.2 cm in diameter).

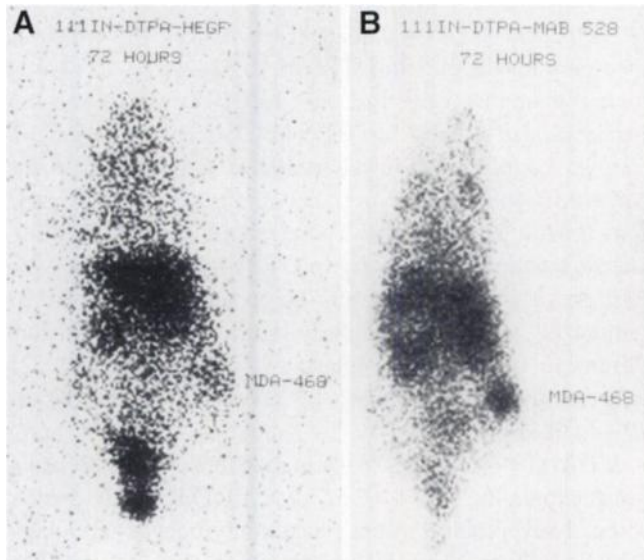


FIGURE 3. Posterior whole-body images of athymic mouse bearing subcutaneous MDA-MB-468 human breast cancer xenograft at 72 h after injection of ^{111}In -DTPA-hEGF (A) or ^{111}In -DTPA-MAb 528 (B). Tumor is visualized with either radiopharmaceutical but is more clearly defined with ^{111}In -DTPA-MAb 528.

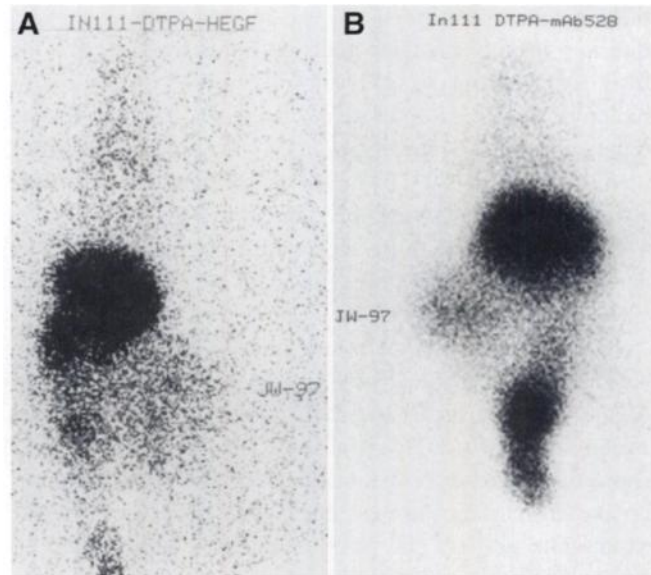


FIGURE 4. Posterior whole-body images of scid mouse bearing subcutaneous JW-97 human breast cancer xenograft at 72 h after injection of ^{111}In -DTPA-hEGF (A) or ^{111}In -DTPA-MAb 528 (B). Tumor is visualized with either radiopharmaceutical but is more clearly defined with ^{111}In -DTPA-MAb 528.

DISCUSSION

Our objective was to compare a peptide-based radiopharmaceutical and a MAb directed against the same cell-surface receptor for imaging of human breast cancer. A systematic evaluation of the localization profiles of these 2 different radiopharmaceuticals was conducted in breast cancer xenografts expressing a broad range of EGFR levels. EGFR-positive breast cancer xenografts hosted in immunocompromised mice were successfully imaged using hEGF, a 53-amino acid peptide ligand (M_r , 6 kDa) for the receptor or anti-EGFR MAb 528 (M_r , 150 kDa) labeled with ^{111}In . The tumor uptake observed with ^{111}In -DTPA-MAb 528 was 7- to 10-fold higher than that observed for ^{111}In -DTPA-hEGF. As a result, the images of the breast cancer xenografts were much clearer with ^{111}In -DTPA-MAb 528, indicating that in certain situations MAbs are more effective tumor-targeting vehicles than are peptide growth factors for receptor imaging of cancer. The higher tumor uptake observed with ^{111}In -DTPA-MAb 528 was likely the result of its slower elimination from the blood, which permitted a greater proportion of the injected dose of the radiopharmaceutical to diffuse into the extravascular space and bind to receptors on breast cancer cells. The higher accumulation of radioactivity in the MDA-MB-468 breast cancer xenografts observed for ^{111}In -DTPA-MAb 528 was not the result of a higher receptor binding affinity, because cell-binding assays showed that the affinity constant for ^{111}In -DTPA-MAb 528 was actually 6-fold lower than that for ^{111}In -DTPA-hEGF ($K_a = 1.2 \times 10^8$ versus 7.5×10^8 L/mol, respectively; Table 1).

^{111}In -DTPA-hEGF was rapidly eliminated from the blood in the animals with <2%–3% of the injected dose remaining in the circulation at 24 h after injection and <1% at 72 h. Two possible mechanisms could explain the rapid blood clearance of ^{111}In -DTPA-hEGF: (a) sequestration by normal tissues that have high levels of EGFR expression (e.g., liver and kidneys), and (b) a high proportion of renal elimination. ^{111}In -DTPA-MAb 528 was eliminated much more slowly from the blood than ^{111}In -DTPA-hEGF, with 25%–30% of the injected dose present in the circulation at 24 h after injection and 10% at 72 h. The slow elimination of ^{111}In -DTPA-MAb 528 from the blood was the result of its large molecular size (M_r , 150 kDa), which prevented its filtration at the glomerulus, a process restricted to proteins with $M_r < 60$ kDa.

Normal hepatocytes exhibit moderate-to-high levels of EGFR expression (8×10^4 – 3×10^5 EGFR/cell) (15,16), and specific receptors for ^{125}I -EGF have been detected in vitro in rat kidney homogenates (17) and on renal tubular cells (18). The liver has also been shown to have a high capacity to extract ^{125}I -EGF from the circulation (16,19). ^{125}I -EGF taken up by hepatocytes is primarily internalized into lysosomes and degraded, but a fraction of internalized EGF molecules are transported by a nonlysosomal pathway and secreted into the bile (19). In this study, the liver and kidneys accumulated the highest concentrations of ^{111}In -DTPA-hEGF and ^{111}In -DTPA-MAb 528. Although ^{125}I -labeled EGF has also been

reported to exhibit high liver and kidney uptake, radioactivity was cleared from these organs within a few hours (20–22). For example, in rats administered ^{125}I -labeled hEGF, >90% of liver radioactivity was cleared within 90 min (19). In contrast, the concentration of ^{111}In radioactivity in the liver and kidneys of mice administered ^{111}In -DTPA-hEGF or ^{111}In -DTPA-MAb 528 remained relatively constant up to 72 h after injection (Fig. 1). The clearance of radioactivity from the liver and kidneys after administration of ^{125}I -labeled hEGF is thought to be the result of binding of the radioligand to cell surface receptors on hepatocytes or renal tubular cells, followed by internalization and degradation to free ^{125}I and ^{125}I -iodotyrosine. These catabolites are then exported from the cells and eliminated (23). ^{111}In -DTPA-hEGF may follow a similar biologic pathway involving its binding and internalization by hepatocytes or renal tubular cells and degradation by intracellular proteases. However, in the case of ^{111}In -DTPA-hEGF, the final catabolites are likely ^{111}In -DTPA covalently linked to 1 of the 2 lysine residues (K_{28} or K_{48}) or to the N-terminal asparagine. These terminal catabolites would not be recognized by amino acid transporters and therefore would be retained within the cells (24). ^{111}In -DTPA-MAb 528 may undergo catabolic fate similar to that of ^{111}In -DTPA-hEGF through its specific binding to cell surface receptors followed by internalization and degradation to catabolites that are retained by cells. Binding of ^{111}In -DTPA-MAb 528 to hepatocytes could be mediated by binding to EGFRs and also to Fc receptors (25).

Because hEGF is a peptide, it is readily filtered at the glomerulus and excreted into the urine. ^{125}I -labeled EGF is cleared from the blood by glomerular filtration and is secreted by the proximal renal tubules after binding to receptors on renal tubular cells (26–28). ^{125}I -labeled EGF is not reabsorbed by the renal tubules (28). It is likely that ^{111}In -labeled hEGF is excreted by a similar mechanism. Renal excretion was the major factor that resulted in the rapid decrease in the blood concentration of ^{111}In -DTPA-hEGF, because sequestration by the liver and kidneys accounted for only 11%–14% and 4%–5% of the injected dose of the radiopharmaceutical, respectively.

Although there was a relatively high accumulation of the radiopharmaceuticals by normal tissues such as the liver and kidneys, both ^{111}In -DTPA-hEGF and ^{111}In -DTPA-MAb 528 localized sufficiently in the MDA-MB-468 and JW-97 human breast cancer xenografts to visualize the tumor by γ scintigraphy at 72 h after injection (Figs. 3 and 4). The images obtained with ^{111}In -DTPA-hEGF and ^{111}In -DTPA-MAb 528 also showed relatively high normal tissue uptake by the liver and kidneys for the reasons discussed, as well as localization of radioactivity in the area of the submaxillary glands. The normal liver and kidney accumulation of both radiopharmaceuticals could limit their clinical usefulness for the detection of liver or adrenal gland metastases in breast cancer patients. The submaxillary glands are responsible for EGF synthesis (29), and it is possible that receptors may be present in these tissues to bind and store the newly synthe-

sized growth factor. EGF conjugated with other radionuclides has also been shown to localize in EGFR-positive tumors. Capala et al. (30) showed that ^{99m}Tc -EGF was selectively retained in the brains of rats inoculated with glioma cells transfected with the EGFR gene but not in normal rats. Rusckowski et al. (31) imaged A431 squamous cell carcinoma xenografts (2×10^6 EGFR/cell) hosted in athymic mice, with ^{99m}Tc -EGF achieving tumor-to-blood ratios of 4:1 at 12 h after injection. Cuartero-Plaza et al. (32) detected squamous cell lung carcinoma in 6 of 9 cancer patients by γ scintigraphy using ^{131}I -EGF. To our knowledge, however, this is the first report of successful imaging of EGFR-positive human breast cancer using ^{111}In -labeled EGF or anti-EGFR MAb 528.

The level of accumulation of ^{111}In -DTPA-MAb 528 (11–22 %ID/g; Fig. 1B) in the MDA-MB-468 and JW-97 tumors was 7- to 10-fold higher than that observed for ^{111}In -DTPA-hEGF, allowing much clearer definition of the tumor despite the slightly lower tumor-to-blood ratios associated with ^{111}In -DTPA-MAb 528 (5:1 versus 12:1; Fig. 2). Goldenberg et al. (33) successfully imaged MDA-MB-468 human breast cancer xenografts using the anti-EGFR MAb 225 (IgG_{2a}) labeled with ^{111}In , but the tumor uptake was more than 5-fold lower than we observed with ^{111}In -labeled MAb 528 (4 versus 22% ID/g). Because ^{111}In labeled MAb 225 has already been shown to successfully image squamous cell lung carcinoma in patients (34), the higher tumor uptake observed with ^{111}In -DTPA-MAb 528 in the MDA-MB-468 human breast cancer xenograft model in this study, is encouraging for the ultimate clinical application of this new radiopharmaceutical for the diagnostic imaging of EGFR-positive breast cancer in humans.

It is interesting to speculate on the reasons why we observed no direct quantitative relationship between the level of receptors measured on the breast cancer cell lines *in vitro* and the level of accumulation of either radiopharmaceutical in the corresponding breast cancer xenografts *in vivo*. This finding was not the result of the inactivation of either hEGF or MAb 528 on radiolabeling with ^{111}In , because cell binding assays showed that both radiopharmaceuticals exhibited their expected receptor binding properties (Table 1). Furthermore, biodistribution studies in animals bearing MDA-MB-468 breast cancer xenografts administered a nonspecific ^{111}In -labeled IgG_{2a} or ^{111}In -DTPA-hEGF mixed with an excess of nonradioactive hEGF (to compete with radiolabeled-hEGF for receptor binding) showed a 2- to 5-fold decrease in tumor uptake, suggesting that the tumor accumulation of the radiopharmaceuticals was receptor mediated.

One possible explanation for our inability to observe a direct correlation between receptor expression levels *in vitro* and tumor uptake of the radiopharmaceuticals *in vivo* is that in the context of tumor-bearing mice, only very small concentrations of the radiopharmaceuticals actually reached the interstitial fluid bathing the cancer cells. Under these conditions, the concentration of EGFRs on the breast cancer

cells may have been in excess and the amount of radioligand would therefore be the limiting factor controlling tumor uptake. For example, based on a tumor uptake of $\sim 2\%$ ID/g (Fig. 1) and an injected dose of $1 \mu\text{g}$ ^{111}In -DTPA-hEGF, there would be $\sim 2 \times 10^{12}$ molecules of the radiopharmaceutical ($0.02 \mu\text{g}$) delivered to 2.5×10^8 MDA-MB-468 breast cancer cells contained in a 1 g breast cancer xenograft (assuming a breast cancer cell with a diameter of $20 \mu\text{m}$). The cells would express a total of 2.5×10^{14} EGFR at an expression level of $\sim 10^6$ EGFR/cell (Table 1) and, therefore, there would be approximately a 100-fold excess of receptors present in the tumor compared with the radioligand. Similarly, for ^{111}In -DTPA-MAb 528, assuming an injected dose of $50 \mu\text{g}$ and a tumor uptake of 15 %ID/g (Fig. 1), there would be $\sim 3 \times 10^{13}$ molecules ($7.5 \mu\text{g}$) of MAb 528 delivered to the tumor. In this case, there would be a 10-fold excess of receptors compared with radioligand. The receptor level on the breast cancer cells was measured *in vitro* by increasing the concentration of radioligand until the concentration of receptors on the cells was the limiting factor. Under these conditions, breast cancer cells with a lower level of receptor expression (e.g., MCF-7 cells) bound less radioligand than cells with a higher level of receptor expression (e.g., MDA-MB-468 cells).

Although, the range of EGFR expression levels on the tumor xenografts studied was not as wide as that in this study, Rusckowski et al. (31) also noted a similar finding using ^{99m}Tc -EGF in athymic mice bearing either A431 squamous cell carcinoma or LS174T colon cancer xenografts. Despite a 6-fold difference in EGFR expression *in vitro* between the A431 and LS174T cells (2×10^6 versus 3.6×10^5 EGFR/cell, respectively), there was no statistically significant difference in tumor uptake *in vivo* (0.4 ± 0.09 versus 0.32 ± 0.06 %ID/g respectively). Senekowitsch-Schmidtke et al. (35) found a partial correlation between tumor uptake and EGFR level in human tumor xenografts implanted into athymic mice using ^{125}I -EGF but not with ^{125}I -labeled anti-EGFR MAb 425. The tumor uptake of ^{125}I -EGF was 2-fold higher in A431 xenografts compared with gastric cancer xenografts, but the A431 tumors expressed an 8-fold higher level of EGFRs. The tumor uptake of ^{125}I -MAb 425 was higher in breast cancer xenografts than in A431 tumors, despite higher EGFR expression by the A431 tumors. The results of this study suggest that the level of tumor localization of receptor-binding radiopharmaceuticals *in vivo* is controlled to a greater extent by their rate of elimination from the blood than by the level of receptor expression on cancer cells, provided that the radiopharmaceutical retains receptor-binding capability and a minimal level of receptors is available for binding. An analogous inverse correlation has also been observed previously between the elimination rate and tumor accumulation of different forms of radiolabeled MAbs (e.g., IgG versus F(ab')₂ versus Fab') (25).

CONCLUSION

The results of this study show that a direct quantitation of the level of receptor expression on cancer cells in vivo by γ scintigraphy may not be possible. Nevertheless, EGFR-positive tumor nodules in mice were detected qualitatively using radiopharmaceuticals that specifically bind to the receptor. Radiolabeled anti-EGFR MAbs would be more effective receptor-binding radiopharmaceuticals for tumor imaging in cancer patients than peptide-based agents, such as hEGF, because the slower elimination rate from the blood leads to higher tumor uptake at only moderately lower tumor-to-blood ratios. Clinical studies with ^{99m}Tc -anti-EGFR MAb ior egf/r3 have demonstrated that EGFR-positive lesions can be detected with high sensitivity in cancer patients (36).

ACKNOWLEDGMENTS

This research was supported in part by grants from DuPont Pharma, the Susan G. Komen Breast Cancer Foundation (grant no. 9749) and the U.S. Army Breast Cancer Research Program (grant no. DAMD17-98-1-8171) and by a grant from the National Cancer Institute of Canada with funds from the Canadian Cancer Society. Parts of this study were presented at the Society of Nuclear Medicine, 45th Annual Meeting, Toronto, Canada, on June 8, 1998.

REFERENCES

1. Klijn JGM, Berns PMJJ, Schmitz PIM, Foekens JA. The clinical significance of epidermal growth factor receptor (EGF-R) in human breast cancer: a review of 5232 patients. *Endocr Rev*. 1992;13:3-17.
2. Mendelsohn J. Epidermal growth factor receptor as a target for therapy with antireceptor monoclonal antibodies. *J Natl Cancer Inst Monogr*. 1992;13:125-131.
3. Fry DW, Kraker AJ, McMichael A, et al. A specific inhibitor of the epidermal growth factor receptor tyrosine kinase. *Science*. 1994;265:1093-1095.
4. Shaw JP, Akiyoshi DE, Arrigo DA, et al. Cytotoxic properties of DAB₄₈₆EGF and DAB₃₈₉EGF, EGF receptor targeted fusion toxins. *J Biol Chem*. 1991;266:21118-21124.
5. Reilly RM, Kiarash R, Cameron RG, et al. ^{111}In -labeled EGF is selectively radiotoxic to human breast cancer cells overexpressing EGFR. *J Nucl Med*. 2000;41:429-438.
6. Andersson A, Capala J, Carlsson J. Effects of EGF-dextran-tyrosine- ^{131}I conjugates on the clonogenic survival of cultured glioma cells. *J Neuro Oncol*. 1992;14:213-223.
7. Kuukasjarvi T, Kononen J, Helin H, Isola J. Loss of estrogen receptor in recurrent breast cancer is associated with poor response to endocrine therapy. *J Clin Oncol*. 1996;14:2584-2589.
8. Fischman AJ, Babich JW, Strauss HW. A ticket to ride: peptide radiopharmaceuticals. *J Nucl Med*. 1993;34:2253-2263.
9. Gill GN, Kawamoto T, Cochet C, et al. Monoclonal anti-epidermal growth factor receptor antibodies which are inhibitors of epidermal growth factor binding and antagonists of epidermal growth factor-stimulated tyrosine protein kinase activity. *J Biol Chem*. 1984;259:7755-7760.
10. Filmus J, Trent JM, Pollak MN, Buick RN. Epidermal growth factor receptor gene-amplified MDA-468 breast cancer cell line and its non-amplified variants. *Mol Cell Biol*. 1987;7:251-257.
11. Reilly RM, Gariépy J. Investigation of factors influencing the sensitivity of tumor detection using a receptor-binding radiopharmaceutical. *J Nucl Med*. 1998;39:1037-1042.
12. Reilly RM, Marks A, Law J, Lee NS, Houle S. In-vitro stability of EDTA and DTPA immunoconjugates of monoclonal antibody 2G3 labeled with In-111. *Appl Radiat Isot*. 1992;43:961-967.
13. Motulsky HJ, Stannard P, Neubig R. *Prism Ver 2.0* [software]. San Diego, CA: GraphPad Software Inc.; 1995.
14. Lindmo T, Boven E, Cuttitta F, Fedorko J, Bunn PA Jr. Determination of the immunoreactive fraction of radiolabeled monoclonal antibodies by linear extrapolation of binding to infinite antigen excess. *J Immunol Methods*. 1984;72:77-89.
15. Dunn WA, Hubbard AL. Receptor-mediated endocytosis of epidermal growth factor by hepatocytes in the perfused rat liver: ligand and receptor dynamics. *J Cell Biol*. 1984;98:2148-2159.
16. Gladhaug P, Christoffersen T. Kinetics of epidermal growth factor binding and processing in isolated intact rat hepatocytes: dynamic externalization of receptors during ligand internalization. *Eur J Biochem*. 1987;164:267-275.
17. Yanai S, Sugiyama Y, Kim DC, et al. Binding of human epidermal growth factor to tissue homogenates of the rat. *Chem Pharmacol Bull*. 1987;35:4891-4897.
18. Fisher DA, Salido EC, Barajas L. Epidermal growth factor and the kidney. *Annu Rev Physiol*. 1989;51:67-80.
19. St. Hilaire RJ, Hradek GT, Jones AL. Hepatic sequestration and biliary secretion of epidermal growth factor: evidence for a high-capacity uptake system. *Proc Natl Acad Sci USA*. 1983;80:3797-3801.
20. De Acosta CM, Justiz E, Skoog L, Lage A. Biodistribution of radioactive epidermal growth factor in normal and tumor bearing mice. *Anticancer Res*. 1989;9:87-92.
21. Scott-Robson S, Capala J, Carlsson J, et al. Distribution and stability in the rat of a $^{76}\text{Br}/^{125}\text{I}$ -labelled polypeptide, epidermal growth factor. *Nucl Med Biol*. 1991;18:241-246.
22. Vinter-Jensen L, Frokiaer J, Jorgensen PE, et al. Tissue distribution of ^{131}I -labelled epidermal growth factor in the pig visualized by dynamic scintigraphy. *J Endocrinol*. 1995;144:5-12.
23. Tyson LM, Browne CA, Jenkin G, Thorburn GD. The fate and uptake of murine epidermal growth factor in the sheep. *J Endocrinol*. 1989;123:121-130.
24. Duncan JR, Welch MJ. Intracellular metabolism of indium-111-DTPA labeled receptor targeted proteins. *J Nucl Med*. 1993;34:1728-1738.
25. Reilly RM, Sandhu J, Alvarez-Diez T, et al. Problems of delivery of monoclonal antibodies: pharmaceutical and pharmacokinetic solutions. *Clin Pharmacokinet*. 1995;28:126-142.
26. Kim DC, Sugiyama Y, Fuwa T, et al. Kinetic analysis of the elimination process of human epidermal growth factor (hEGF) in rats. *Biochem Pharmacol*. 1989;38:241-249.
27. Jorgensen PE, Poulsson SS, Nexø E. Distribution of intravenously administered epidermal growth factor in the rat. *Regulatory Peptides*. 1988;23:161-169.
28. Nielsen S, Nexø E, Christensen EI. Absorption of epidermal growth factor and insulin in rabbit renal proximal tubules. *Am J Physiol*. 1989;256:E55-E63.
29. Carpenter G, Cohen S. Epidermal growth factor. *Ann Rev Biochem*. 1979;48:193-216.
30. Capala J, Barth RF, Bailey MQ, Fenstermaker RA, Marek M, Rhodes, BA. Radiolabeling of epidermal growth factor with ^{99m}Tc and in vivo localization following intracerebral injection into normal and glioma-bearing rats. *Bioconjug Chem*. 1997;8:289-295.
31. Ruszkowski M, Qu T, Chang F, Hnatowich DJ. Technetium-99m labeled epidermal growth factor-tumor imaging in mice. *J Peptide Res*. 1997;50:393-401.
32. Cuartero-Plaza A, Martinez-Mirallas E, Rosell R, Vadell-Nadal C, Farre M, Real FX. Radiolocalization of squamous lung carcinoma with ^{131}I -labeled epidermal growth factor. *Clin Cancer Res*. 1996;2:13-20.
33. Goldenberg A, Masui H, Divgi C, et al. Imaging of human tumor xenografts with an indium-111-labeled anti-epidermal growth factor receptor monoclonal antibody. *J Natl Cancer Inst*. 1989;81:1616-1625.
34. Divgi CR, Welt S, Kris M. Phase I and imaging trial of indium-111 labeled anti-EGF receptor monoclonal antibody 225 in patients with squamous cell lung carcinoma. *J Natl Cancer Inst*. 1991;83:97-104.
35. Senekowitsch-Schmidtke R, Steiner K, Haunschild J, Mollenstadt S, Truckenbrodt R. In vivo evaluation of epidermal growth factor (EGF) receptor density on human tumor xenografts using radiolabeled EGF and anti-(EGF receptor) mAb 425. *Cancer Immunol Immunother*. 1996;42:108-114.
36. Ramos-Suzarte M, Rodríguez N, Oliva JP, et al. ^{99m}Tc -labeled antihuman epidermal growth factor receptor antibody in patients with tumors of epithelial origin: part III. Clinical trials safety and diagnostic efficacy. *J Nucl Med*. 1999;40:768-775.